Polar Enhanced Resolution Freeze/Thaw Data Record from AMSR-E and AMSR2

Version 1.0

Contact Information:

Youngwook Kim, John S. Kimball, Jinyang Du. and Tobias Kundig

Numerical Terradynamic Simulation Group (NTSG)

The University of Montana

Missoula MT, 59812

Email: john.kimball@umontana.edu; youngwook.kim@umontana.edu;

Jinyang.du@umontana.edu; tobias.kundig@umconnect.umt.edu

Project URL: http://freezethaw.ntsg.umt.edu/

Release date: 2018-12-10T19:23

The following reference should be used to cite these data:

Kim, Y., J. S. Kimball, J. Du, and J. Glassy. 2017. Polar Enhanced Resolution Freeze/Thaw Data Record from AMSR-E and AMSR2, Version 01 [2002 to 2016]. Boulder Colorado USA: National Snow and Ice Data Center. Digital media (https://doi.org/10.5067/WM9R9LQ2SA85).

The following peer-reviewed citation describes FT-ESDR science algorithms, accuracy and performance:

Kim, Y., J. S. Kimball, J. Glassy, and J. Du. (2017). An Extended Global Earth System Data Record on Daily Landscape Freeze-Thaw Determined from Satellite Passive Microwave Remote Sensing, *Earth System Science Data*, 9 (1), 133-147.

Acknowledgements: These data were generated through a grant from the NASA MEaSUREs (Making Earth System Data Records for Use in Research Environments) program (NNX14AB20A). This work was conducted at the University of Montana under contract to NASA.

Contents:

I. Introduction ……………………………………………………………………………2

II. Data description …………………………………………………………………………2

III. PER FT-ESDR version 1.0 protocols ..……...………………..………………………4

IV. PER FT-ESDR accuracy and performance …...…………………………...………5

V. FT algorithms …………………………………….…………………………………...6

VI. Ancillary data for PER FT-ESDR ……………………………………………………7

VII. Hierarchical data archive structure and available software tools …………………....9

VIII. Data format and file naming convention ……………………………………………10

IX. Data organization and volume ………………………..………………………...11

X. Example FT figures …………………………………….……………………...13

XI. References ………………………………………….…………………………………14

I. Introduction:

This document describes a northern hemisphere Polar Enhanced Resolution (PER) data record of daily landscape Freeze/Thaw (FT) status derived at 6-km resolution from satellite passive microwave remote sensing. The PER FT regional data record augments an existing global 25-km resolution FT Earth System Data Record (FT-ESDR) (Kim et al., 2017a). The FT state parameter quantifies the predominant frozen or non-frozen state of the landscape and is closely linked to changes in the surface energy budget and evapotranspiration (Kim et al., 2018; Zhang et al. 2011), vegetation growth and phenology (Kim et al., 2014b), snowmelt dynamics (Kim et al., 2015), permafrost extent and stability (Park et al., 2016), terrestrial carbon budgets and land-atmosphere trace gas exchange (Kim et al., 2014a). Satellite microwave remote sensing is well suited for global FT monitoring due to its relative insensitivity to atmospheric contamination and solar illumination effects, and strong microwave sensitivity to changes in surface dielectric properties between frozen and non-frozen conditions.

II. Data description

The northern hemisphere Polar Enhanced Resolution (PER) FT Earth System Data Record (FT-ESDR) was primarily derived using similar calibrated overlapping daily [morning (AM) and afternoon (PM) overpass] radiometric brightness temperature (T_b) measurements at 36.5 GHz (V-pol) frequency from the NASA Advanced Microwave Scanning Radiometer for EOS (AMSR-E) and the JAXA Advanced Microwave Scanning Radiometer 2 (AMSR2) series. The resulting PER FT-ESDR represents a consistent, daily FT polar record that extends over a 16 year (2002 to 2017) observation period, ensuring cross-sensor consistency through double-differencing calibration of AMSR2 to AMSR-E T_b records (Du et al., 2014). Double-differencing calibration was conducted using similar frequency collocated overlapping T_b records from the FY-3B Microwave Radiation Imager (MWRI), which was applied to fill the temporal T_b gaps for 2011-2012 period (Du et al., 2014). The MWRI on the Chinese FengYun 3B (FY3b) satellite was launched in November 2010 (Yang et al., 2011) and has similar instrument configuration and data acquisition times as the AMSR-E and AMSR2 (hereafter AMSR) sensors.

Calibrated T_b data records from the AMSR sensors were used to develop a daily PER FT-ESDR over the northern hemisphere (NH) domain. The 6-km resolution of the PER FT product grid provides approximately four-fold improved spatial resolution over the global 25-km resolution FT-ESDR product and is enabled by processing of orbital swath T_b retrievals closer to the native AMSR 36.5 GHz sensor footprint. The AMSR-E 36.5 GHz orbital swath T_b data have a native footprint resolution of 14km x 8km (Kawanishi et al., 2003), while the similar frequency T_b orbital swath (L1R) data from AMSR2 has a native 12km x 7km footprint resolution (Imaoka et al., 2010, 2012). The AMSR swath T_b data were re-projected to a 6-km polar EASE-Grid 2.0 projection format (Brodzik et al., 2014) using an Inverse Distance Squared spatial interpolation approach following previously established methods (Du et al., 2017). Detailed descriptions of the FT-ESDR methods, algorithm performance and product accuracy are provided by Kim et al. (2017a).

The FT-ESDR is intended to have sufficient accuracy, resolution, and coverage to resolve physical processes linking Earth's water, energy and carbon cycles. The product is designed to determine the FT status of the composite landscape vegetation-snow-soil medium to a sufficient level to characterize the frozen temperature constraints to surface water mobility, vegetation productivity, ecosystem respiration and land-atmosphere carbon (CO_2) fluxes. The FT-ESDR utilizes a daily binary FT state classification on a grid cell-by-cell basis, posted to a polar 6-km Earth grid. The FT classification algorithm uses a temporal change detection of radiometric T_b time-series that identify FT transition sequences by exploiting the dynamic temporal T_b response to differences in the aggregate landscape dielectric constant that occur as the landscape transitions between predominantly frozen and non-frozen conditions (McDonald and Kimball 2005; Kim et al., 2011, 2012). Satellite ascending and descending orbital T_b time series are processed separately to produce information on AM, PM and composite daily FT conditions (CO). Additional variables distinguished by the FT-ESDR include transitional (AM frozen and PM thawed) or inverse transitional (AM thawed and PM frozen) conditions. **Table 2** describes the file encoding of FT-ESDR pixel values corresponding to frozen, thawed, and transitional conditions. The PER FT-ESDR domain encompasses all NH land areas affected by seasonal frozen temperatures, including urban, barren land, snow-ice and open water body dominant grid cells (Kim et al., 2017a).

Both PER and global FT-ESDR data records are available for public access via FTP download through the FT-ESDR project web site (http://freezethaw.ntsg.umt.edu) and NTSG HTTP Data Service (http://files.ntsg.umt.edu/data/FT_ESDR_PER/), and through the NASA DAAC at the National Snow and Ice Data Center (https://nsidc.org/data/nsidc-0728); these data include a variety of file formats including Geotiff and searchable metadata. The FT-ESDR is projected in a polar cylindrical Equal-Area Scalable Earth (EASE) grid, Version 2 format (Brodzik et al., 2014) consistent with the format of the underlying AMSR polar T_b records used as primary inputs for the FT classification.

III. PER FT-ESDR version 1.0 protocols

The Version 1.0 product contains similar protocols used to construct baseline global FT-ESDR product version 4.0 (Kim et el. 2017a):

- A long-term FT data record is represented, extending over the combined calibrated AMSR (AMSR-E and AMSR2) period of record from 2002 to 2017 (16-years);

- The PER FT-ESDR domain encompasses all NH land areas affected by seasonal frozen temperatures, including urban, snow-ice dominant, open water body dominant, and barren land. Open water areas included in the FT classification represent grid cells where the fractional surface water (*fw*) cover is less than 100% of the cell;
- A modified seasonal threshold algorithm (MSTA) is used for the FT classification where MSTA T_b reference FT conditions are calibrated annually for each pixel using 6-km resolution daily surface air temperature (SAT) records downscaled from coarser resolution (0.25°) ERA-Interim reanalysis data (Dee et al., 2011) using temperature lapse rates defined from an Aqua MODIS LST climatology and digital elevation map;
- Detailed quality control (QC) flags are included in the product granules identifying grid cells and days with missing and interpolated T_b observations, and characterizing extensive open water bodies, complex terrain, and precipitation events;
- Updated annual data quality assurance (QA) maps are included indicating product performance and reliability.

The Version 1.0 PER FT-ESDR has greater spatial coverage than earlier global FT-ESDR versions (Kim et al., 2014c), especially over boreal and arctic land areas with extensive open water cover that were previously screened from earlier FT classifications (Kim et al. 2011). Changes from the baseline global FT-ESDR Version 4.0 data include a finer spatial resolution (6km) FT data records and NH polar EASE-grid 2.0 format, which reduces spatial distortion of FT grid cells at higher latitudes relative to the global FT-ESDR product.

IV. FT-ESDR accuracy and performance

The Version 1.0 PER FT-ESDR release is developed by merging AMSR-E and AMSR2 36.5 GHz frequency, vertical (V) polarization T_b records, and applying similar protocols used to construct earlier FT-ESDR product versions (Kim et el. 2011, 2012, 2014c). The PER FT-ESDR extends from 2002 to 2017 over a NH classification domain and has been verified against a range of other independent FT metrics, including daily surface air temperature (SAT) records from NH weather stations (Kim et al., 2017a). The FT-ESDR product accuracy is primarily assessed in relation to daily SAT maximum (SAT_{max}) and minimum (SAT_{min}) values from the NH WMO weather station network (4862±458 [temporal-SD] stations); mean annual FT spatial classification accuracies are approximately 93.0 ±0.4 [inter-annual SD] and 85.9±0.9 [inter-annual SD] percent for respective PER FT PM and AM retrievals over the NH domain and long-term record. The PER FT classification accuracy shows strong seasonal and annual variability, and is generally lower during active FT transition periods when spatial heterogeneity in landscape FT processes is maximized (Kim et al. 2017a). NH daily FT spatial classification accuracy is defined for each product daily granule from pixel-wise comparisons of FT classification accuracy in relation to co-located NH weather station network daily air temperature (SAT_{min}, SAT_{max}) measurements (Kim et al. 2017a); spatial classification accuracy is expressed as the proportion of NH stations where the daily FT classification is consistent with station SAT measurement based FT estimates. Other data quality (QA) metrics are included that provide more spatially explicit information on algorithm performance, including potential negative impacts from open water cover, terrain complexity, length of FT transitional season, and MSTA FT threshold uncertainty influencing mean annual classification accuracy. Additional quality control (QC) flags identify other factors potentially affecting FT classification accuracy. The QC flags are spatially and temporally dynamic, and assigned on a per grid cell basis to denote missing satellite T_b records that are subsequently gap-filled through temporal interpolation of adjacent successful T_b retrievals prior to the FT classification. The QC flags also distinguish grid cells with large fractional open water areas (fw>0.20) and extreme elevation gradients (>300m), and days with large precipitation events (Ferraro et al., 1996).

V. FT algorithms:

The PER FT-ESDR classification involves a modified seasonal threshold algorithm approach (MSTA) with radiometric T_b time-series that identify FT transition sequences by exploiting the dynamic T_b temporal response to differences in the aggregate landscape dielectric constant that occur as the landscape transitions between predominantly frozen and non-frozen conditions. These techniques are well-suited for resolving daily FT state dynamics rather than single events or seasonally dominant transitions (Kim et al. 2011). The Version 1.0 product uses the MSTA to classify daily (AM and PM) FT status from 36.5 GHz (V-pol) T_b time series from the AMSR records. The MSTA FT threshold established for each grid cell is defined annually using an empirical linear regression relationship between the satellite T_b retrievals and daily 6-km SAT downscaled from coarser (0.25 degree) spatial resolution ERA-Interim (Dee et al., 2011) global reanalysis daily surface temperature data using a digital elevation map (DEM: Hasting et al., 1999) and an annual mean environmental lapse rate (ELR). The daily grid cell-wise ELR was derived from the linear regression relationship between DEM elevations and MODIS Aqua land surface temperatures (LST) (Kim et al., 2017b). The FT thresholds were derived separately for the satellite T_b time series from AM and PM overpasses and using corresponding daily SAT minimum (SAT_{min}) and maximum (SAT_{max}) values. Larger weighting of SAT values closer to 0°C was used in selecting the corresponding T_b based FT threshold for each grid cell; weighting of the SAT and T_b regression relationship was derived using a cosine function within a temperature range extending from -60.0°C to 30.0°C and representing 99 percent of the SAT frequency distribution defined from the 36-year ERA-Interim SAT global climatology (Kim et al., 2017a). An advantage of the MSTA relative to an earlier seasonal threshold algorithm (STA) based FT classification (Kim et al. 2011) is that the T_b threshold selection does not depend on frozen and non-frozen reference states derived by averaging T_b measurements over respective winter and summer periods, and is less sensitive to T_b data gaps during these reference periods.

VI. Ancillary data used for the FT-ESDR

We used daily SAT records from ERA-Interim model reanalysis for pixel-wise annual calibration the MSTA FT thresholds. The reanalysis data were also used to define the polar FT-ESDR domain (**Figure 1**) using a simple SAT driven bioclimatic index (Kim et al. 2011) that identified all land areas where seasonally frozen air temperatures are a major constraint to ecosystem processes and land surface water mobility.

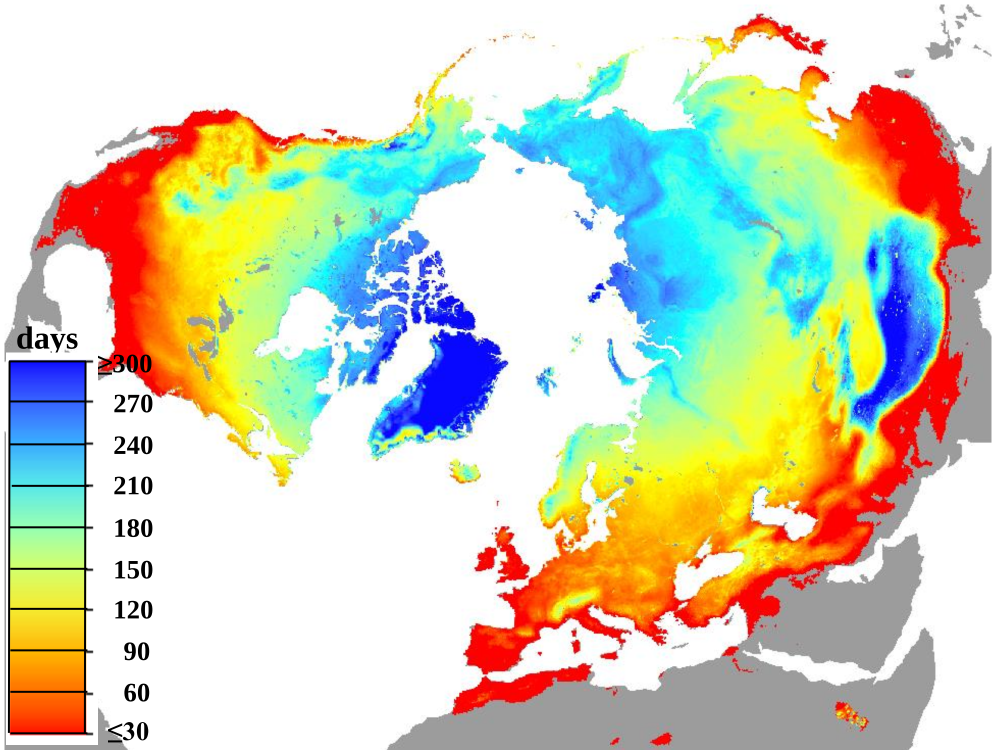

Figure 1*: Mean annual frozen season (frozen or transitional status) over the 15-year (2002-2014) record and Polar FT-ESDR domain; white and grey colors denote respective open water bodies and land areas outside of the FT-ESDR domain.*

Independent daily SAT observations from NH in situ WMO weather station measurements were used for verification of FT-ESDR daily accuracy. A simple zero degree Celsius temperature threshold was used to classify frozen and non-frozen temperatures from the SAT measurements; these results were then compared against the FT-ESDR daily classification results from the overlying grid cell. The resulting NH FT spatial classification accuracy from all WMO stations was then summarized on a daily basis.

A polar QA map is defined for each year of record and provides a discrete, grid cell-wise indicator of relative FT-ESDR quality that accounts for potential negative impacts from open water cover, terrain complexity, length of FT transitional season, and MSTA FT threshold uncertainty influencing mean annual FT classification accuracy indicated from the WMO station comparisons. The resulting annual QA map for selected year 2012 is presented in **Figure 2** and shows regions of relative high to low quality. The QA values were stratified into a smaller set of discrete categories ranging from low (estimated mean annual FT classification accuracy < 70%) to best (> 90%) quality. Mean proportions of the four QA categories encompass 66.9% (best), 22.3% (good; 80-90% agreement), 4.3% (moderate; 70-80% agreement), and 6.4% (low) of the polar FT-ESDR domain for 2012.

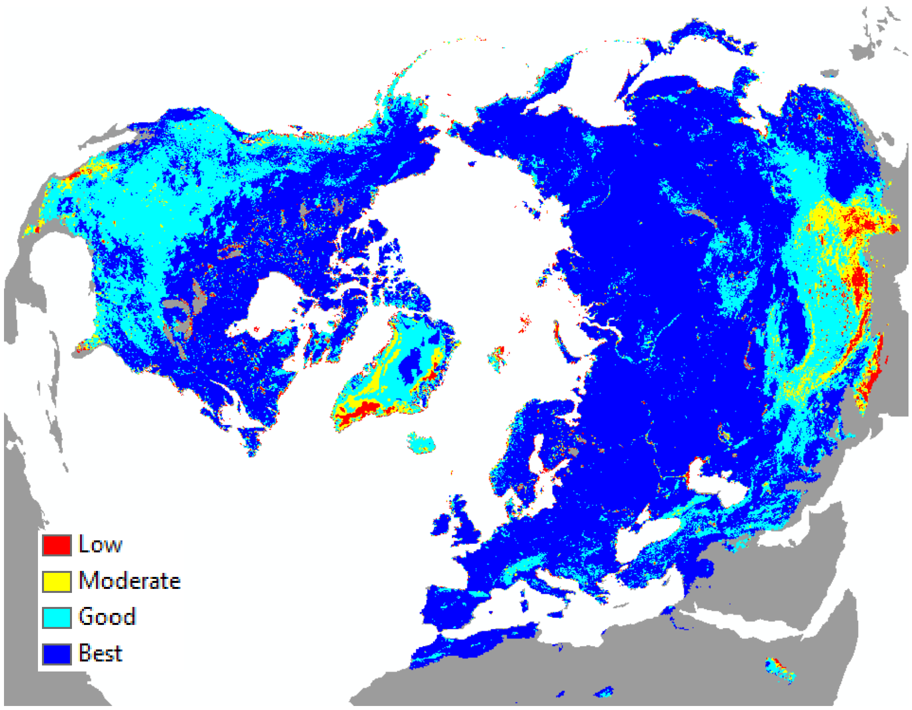

***Figure 2**: FT-ESDR annual quality assurance (QA) map for 2012, aggregated into low (estimated mean annual spatial classification agreement < 70%), moderate (70-80%), good (80-90%) and best (>90%) relative quality categories. Land areas outside of the FT-ESDR domain are denoted by grey shading.*

VII. Hierarchical data archive structure and available software tools:

Prior University of Montana FT-ESDR deliveries consisted of the data hosted on an NTSG FTP service. This PER FT-ESDR 1.0 delivery consists of a set of "tar" archive files, intended for NASA NSIDC personnel to use in constructing a data distribution point at NSIDC. The tar archives and related delivery files consist of the following files as documented in **Table 1** below. The data includes NH daily FT classification files in HDF5 and GeoTIFF formats; daily FT accuracy and annual QA maps, and supporting FT-ESDR documentation and software tools.

Table 1. Tar archive files encompassing the PER FT-ESDR (1.0) delivery.

PER FT-ESDR 1.0 Summary of NTSG Data Service Site	
[1]Directory	Summary of Contents
DAILY_ BINARY	Multi-year record of polar daily binary granules
QA_ACCURACY	Daily FT-ESDR mean polar classification accuracy (%) and annual QA metadata in HDF5 file formats
TAR_ARCHIVES	Compressed tar files (*.tar.gz) FT gridded (global EASE-grid) data files archive for distribution and network transfer
MD5	MD5 checksum hash signatures for each FT file in the collection
DOC	FT-ESDR database documentation files
TOOLS	File viewing software, including Panoply (v3.1.5) and HDFView (v2.8) for HDF5 (on MacOS,windows, Linux platforms)

[1]*Note that within a given directory tree such as DAILY_HDF5, where there is sub-tree for a series of year-wise directories (2002-2016).*

Two commonly available software tools are available through the FT-ESDR project web site and are routinely used with the GeoTIFF file formats this FT-ESDR distribution is produced in; these are HDFView and Panoply. Of course, other tool environments are also commonly used, such as ArcGIS, IDL/ENVI, MatLAB, as well as “R” (rhdf) and various Python implementations (e.g. h5py and GDAL for Python) that support user developed code. Users of the HDF Groups hdfview utility should consult the following URL for additional information regarding their specific platform since there are distinctions in the binary distributions offered based on the user’s operating system (e.g. whether it is 32 or 64 bit, etc.):
https://support.hdfgroup.org/products/java/release/download.html

VIII. Data format and file naming convention:

Each FT-ESDR grid cell is projected in a polar EASE-Grid 2.0 format (Brodzik et al., 2014) at 6-km spatial resolution, with 3000 columns and 3000 rows consisting of 8-bit byte data type, for a total of 9000000 pixels per daily data product. An ESRI projection file is included with the GeoTIFFs to aid in viewing the data in ArcMap. The geographical range of the FT-ESDR product is NH, extending from -179.9999^{o} to 179.9999 ^{o} longitude and from 0^{o} to 90.0^{o}N latitude.

Each daily FT file consists of 3 separate granules, including: morning overpass (AM), afternoon overpass (PM) and combined daily AM and PM (CO) classification results. The FT product naming protocol follows these conventions:

[InstrumentLabel]_[Channel][Polarization]_[OverpassCode]_FT_[Year]_day[DOY]_NH_06km.bin

For example, the file "AMSR_36V_CO_FT_2016_day365_NH_06km.bin" represents AMSR sensor, 37 GHz, vertically polarized T_b based FT classification for composite daily conditions for day (calendar year) 365 over the NH domain and at 6-km spatial resolution.

IX. Data Organization and Volume:

The daily FT data is organized in this collection first by instrument label, and then by year, with the AM, PM and CO granules stored in each annual directory. The FT-ESDR file sizes vary depending on the particular format option selected (**Table 2**). In addition to the primary FT data, detailed product quality information is also provided that includes granule level total mean spatial classification accuracy for the NH domain defined on a daily basis (defined from pixel-wise comparisons against co-located global weather station SAT observations), and spatially contiguous relative data quality (QA) maps updated for each annual cycle. The PER FT-ESDR consists of a total of 16218 daily NH 6km resolution granules, for a total of 137 Gb (Geotiff form) for all FT products. For faster downloading, compressed ("gzip") yearly FT binary files are provided in the "DAILY_TAR_ARCHIVES" directory.

Table 2. FT-ESDR file size summaries for Geotiff files.

Instrument	N. files	Range of Years	GeoTiff Files	
			Kb	Gb
AMSR-E and AMSR2	16218	2002 – 2017	137550000 Kb	137 Gb

A number of compressed tar archives (**Table 3**) are also available (see DAILY_TAR_ARCHIVES directory) as a convenient method for users to access related collections of the FT- ESDR files. Their names, manifests (table of content files), number of files, and data volume sizes are documented in the table below:

Table 5. FT-ESDR compressed tar file (tar.gz) archives and file sizes available for download.

Tar Archive Name	N. Files	Size
FT_V4_AMSR_2002_2017_GeoTIFF.tar.gz	16425	3 Gb
FT_V4_ANNUAL_QA.tar.gz	16	97 Mb

X. Example FT Figures:

The FT-ESDR provides a daily (CO) classification of the predominant landscape frozen or non-frozen status for each grid cell within the NH domain (**Figure 3**). Four discrete FT metrics are distinguished from the AM and PM T_b retrievals, including frozen (both AM and PM overpasses), non-frozen (AM and PM), transitional (AM frozen, PM non-frozen) and inverse-transitional (AM non-frozen, PM frozen) states.

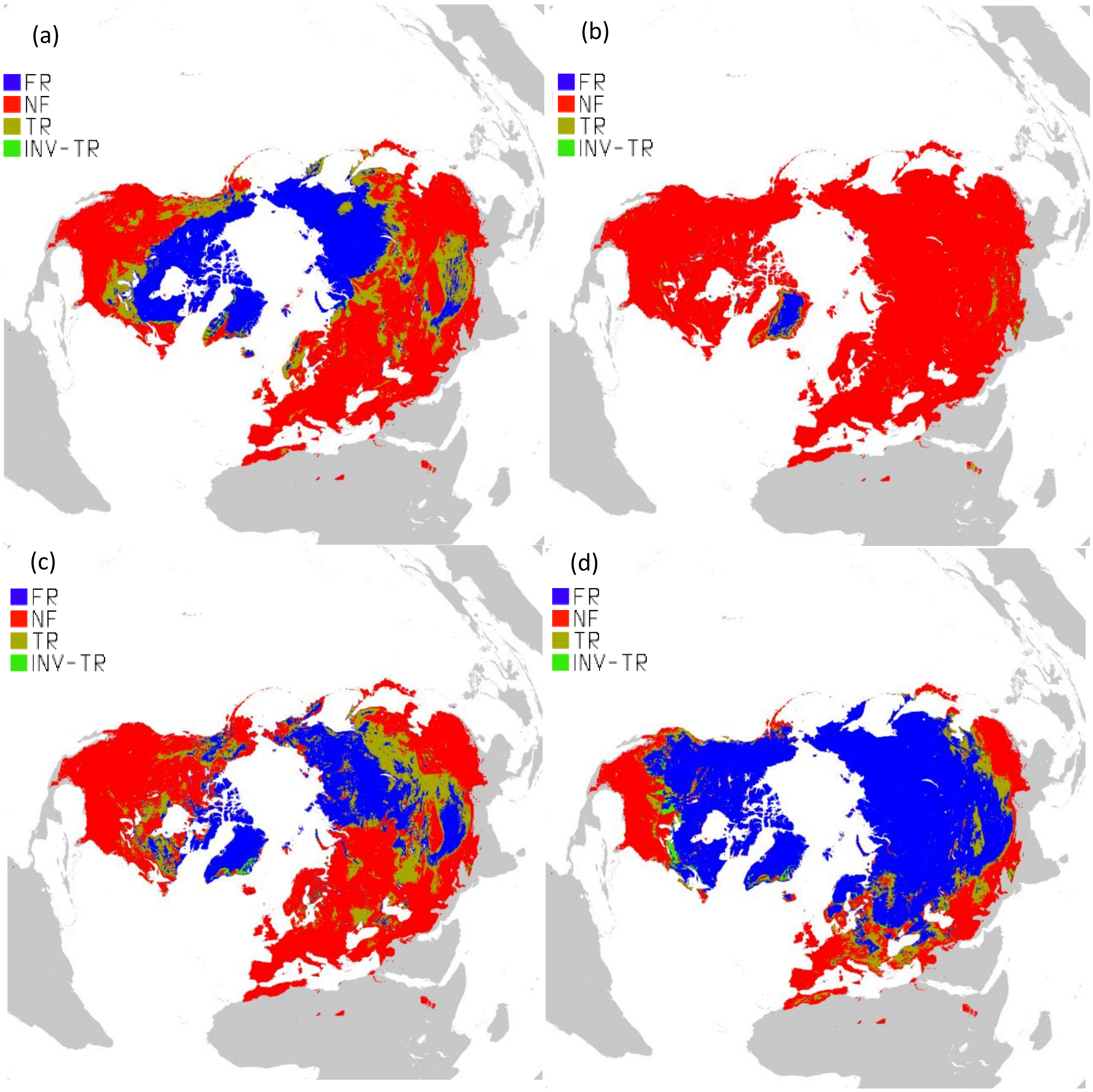

***Figure 3**: Selected daily combined (CO) FT-ESDR classification results for 2016, where: (a) DOY (Day of Year) =100, (b) DOY=200, (c) DOY=300, and (d) DOY=360; white and grey colors denote respective open water bodies and land areas outside of the FT-ESDR domain; FR (AM and PM frozen), NF (AM and PM thawed), TR (AM frozen and PM thawed) and INV-TR (AM thawed and PM frozen).*

XI. References:

Armstrong, R. L. and M. J. Brodzik. 1995. An Earth-Gridded SSM/I Data Set for Cryosphere Studies and Global Change Monitoring. *Advances in Space Research*. 16, 155-163.

Armstrong, R., K. Knowles, M. Brodzik, and M.A. Hardman, 1998, updated 2012. DMSP SSM/I-SSMIS Pathfinder Daily EASE-Grid Brightness Temperatures. Version 2 [1987-2012]. Boulder, Colorado USA: NASA DAAC at the National Snow and Ice Data Center (http://nsidc.org/data/nsidc-0032.html).

Brodzik, M. J., B. Billingsley, T. Haran, B. Raup and M. H. Savorie. 2014. Correction: Brodzik, M. J. et al. EASE-Grid 2.0: Incremental but significant improvements for Earth-Gridded Data sets. *ISPRS International Journal of Geo-Information*, 3 (3), 1154-1156

Brodzik, M. J. and R. L. Armstrong. 2002. EASE-Grid: A versatile set of equal-area projections and grids. In M. Goodchild (Ed.), Discrete Global Girds. Santa Barbara, California USA: National Center for Geographic Information and Analysis.

Dee, D. P., S. M. Uppala, A. J. Simmons, P. Berrisford, P. Poli, S. Kobayashi, U. Andrae, M. A. Balmasewda, G. Balsamo, P. Bauer, P. Bechtold, A. C. M. Beljaars, L. van de Berg, J. Bidlot, N. Bormann, C. Delsol, R. Dragani, M. Fuentes, A. J. Geer, L. Haimberger, S. B. Healy, H. Hersbach, E. V. Holm, L. Isaksen, P. Kallberg, M. Kohler, M. Matricardi, A. P. McNally, B. M. Monge-Sanz, J. J. Morcrette, B. K. Park, C. Peubey, P. de Rosnay, C. Tavolato, J. N. Thepaut, and F. Vitart. (2011). The ERA-Interim reanalysis: configuration and performance of the data assimilation system. *Quarterly Journal of the Royal Meteorological Society*, 137, 553-597

Du, J., J. S. Kimball, C. Duguay, Y. Kim, and J. D. Watts. (2017). Satellite microwave assessment of Northern Hemisphere lake ice phenology from 2002 to 2015. *The Cryosphere*, 11, 47-63

Du, J., J. S. Kimball, and L. Jones. (2015). Satellite Microwave Retrieval of Total Precipitable Water Vapor and Surface Air Temperature Over Land from AMSR2. *IEEE Transactions on Geoscience and Remote Sensing*, 53 (5), 2520-2531

Du, J., J. S. Kimball, J. Shi, L. A. Jones, S. Wu, R. Sun, and H. Yang. (2014). Inter-calibration of satellite passive microwave land observations from AMSR-E and AMSR2 using overlapping FY3B-MWRI sensor measurements. *Remote Sensing*, 6, 8594-8616

Ferraro, R. R., F. Weng, N. C. Grody, and A. Basist. (1996). An eight-year (1987-1994) time series of rainfall, clouds, water vapor, snow cover, and sea ice derived from SSM/I measurements. *Bulletin of the American Meteorological Society*, 77(5), 891-905

Friedl, M. A., D. K. McIver, J. C. F. Hodges, X. Y. Zhang, D. Muchoney, A. H. Strahler, C. E. Woodcock, S. Gopal, A. Schneider, A. Cooper, A. Baccini, F. Gao, and C. Schaaf (2002). Global land cover mapping from MODIS: algorithms and early results. *Remote Sensing of Environment*, 83, 287-302

GLOBE Task Team and others (Hasting, D. A., P. K. Dunbar, G. M. Elphingstone et al.). (1999). The global land one-kilometer base elevation (GLOBE) digital elevation model, version 1.0. National Oceanic and Atmospheric Administration, National Geophysical Data Center, 325

Broadway, Boulder, Colorado 80305-3328, U.S.A. Digital data base on the World Wide Web (http://www.ngdc.noaa.gov/mgg/toto/globe.html) and CD-ROMs.
Imaoka, K.; Takashi, M.; Misako, K.; Marehito, K.; Norimasa, I.; Keizo, N. (2012). Status of AMSR2 instrument on GCOM-W1, earth observing missions and sensors: Development, implementation, and characterization II. Proc. SPIE 2012, 852815, doi:10.1117/12.977774
Imaoka, K., M. Kachi, M. Kasahara, N. Ito, K. Nakagawa, and T. Oki. 2010. Instrument performance and calibration of AMSR-E and AMSR2, ISPRS Archives, 38 (8), 13-18
JAXA. Digital media (https://gcom-w1.jaxa.jp).
Jones, L.A., and J.S. Kimball, 2010, updated 2012. Daily Global Land Surface Parameters Derived from AMSR-E, Version 1.1. Boulder Colorado USA: National Snow and Ice Data Center. Digital media (http://nsidc.org/data/nsidc-0451.html).
Kawanishi, T. J., T. Sezai, Y. Ito, K. Imaoka, T. Takashima, Y. Ishido, A. Shibata, M. Miura, H. Inahata, and R. W. Spencer. (2003). The advanced scanning microwave radiometer for the EarthObserving System (AMSR-E): NASDA's contribution to the EOS for global energy and water cycle studies. *IEEE Transactions on Geoscience and Remote Sensing*, 41 (2), 184-194
Kim, Y., J. S. Kimball, J. Du, C. L. B. Schaaf, and P. B. Kirchner. (2018). Quantifying the effects of freeze-thaw transitions and snowpack melt on land surface albedo and energy exchange over Alaska and Western Canada, Environmental Research Letters, 13 (7), 1-14
Kim, Y., J. S. Kimball, J. Glassy, and J. Du. (2017a). An Extended Global Earth System Data Record on Daily Landscape Freeeze-Thaw Determined from Satellite Passive Microwave Remote Sensing, *Earth System Science Data*, 9 (1), 133-147
Kim, Y., J.S. Kimball, & J. Du. (2017b). Chapter 8. Satellite microwave remote sensing of landscape freeze-thaw status related to frost hazard monitoring . *Remote Sensing of Hydro-Meteorological Hazards* (Boca Raton, FL: CRC Press).
Kim, Y., J. S. Kimball, D. A. Robinson, and C. Derksen. (2015). New satellite climate data records indicate strong coupling between recent frozen season changes and snow cover over high northern latitudes. *Environmental Research Letters*, 10, 084004.
Kim, Y., J. S. Kimball, K. Zhang, K. Didan, I. Velicogna, and K. C. McDonald (2014a). Attribution of divergent northern vegetation growth responses to lengthening non-frozen seasons using satellite optical-NIR and microwave remote sensing, *International Journal of Remote Sensing*, 10.1080/01431161.2014.915595
Kim, Y., J. S. Kimball, K. Didan, and G. M. Henebry. (2014b). Responses of vegetation growth and productivity to spring climate indicators in the conterminous Unites States derived from satellite remote sensing data fusion. *Agricultural and Forest Meteorology*, 194, 132-143
Kim, Y., J. S. Kimball, J. Glassy, and K. C. McDonald (2014c). MEaSUREs Global Record of Daily Landscape Freeze/Thaw Status. Version 3. [1979-2011]. Boulder, Colorado USA: NASA DAAC at the National Snow and Ice Data Center. http://dx.doi.org/10.5067/MEASURES/CRYOSPHERE/nsidc-0477.003
Kim, Y., J.S. Kimball, K. Zhang, and K.C. McDonald, 2012. Satellite detection of increasing northern hemisphere non-frozen seasons from 1979 to 2008: Implications for regional vegetation growth. *Remote Sensing of Environment* 121, 472-487.

Kim, Y., J. S. Kimball, K. C. McDonald, and J. Glassy. 2011. Developing a Global Data Record of Daily Landscape Freeze/Thaw Status using Satellite Microwave Remote Sensing. *IEEE Transactions on Geoscience and Remote Sensing*. 49, 3, 949-960.

Knowles, K., M. Savoie, R. Armstrong, and M. Brodzik, 2006, updated 2011. AMSR-E/Aqua Daily EASE-Grid Brightness Temperatures [2002-2011]. Boulder, Colorado USA: NASA DAAC at the National Snow and Ice Data Center (http://nsidc.org/data/nsidc-0301.html).

Knowles, K., E.G. Njoku, R. Armstrong, and M. Brodzik, 2000. Nimbus-7 SMMR Pathfinder Daily EASE-Grid Brightness Temperatures [1979-1987]. Boulder, Colorado USA: NASA DAAC at the National Snow and Ice Data Center (http://nsidc.org/data/nsidc-0071.html).

McDonald, K.C, and J.S. Kimball, 2005. Hydrological application of remote sensing: Freeze-thaw states using both active and passive microwave sensors. Encyclopedia of Hydrological Sciences. Part 5. Remote Sensing. M.G. Anderson and J.J. McDonnell (Eds.), John Wiley & Sons Ltd. DOI:10.1002/0470848944.hsa059a.

Park, H., Y. Kim, and J. S. Kimball. (2016). Widespread permafrost vulnerability and soil active layer increases over the high northern latitudes inferred from satellite remote sensing and process model assessments. *Remote Sensing of Environment*, 175, 349-358.

Yang, H., F. Weng, L. Lv, N. Lu, G. Liu, M. Bai, Q. Qian, J. He, H. Xu. (2011) The FengYun-3 microwave radiation imager on-orbit verification. *IEEE Transactions on Geoscience and Remote Sensing*, 49, 4552–4560.

Zhang, K., J.S. Kimball, Y. Kim, and K.C. McDonald, 2011. Changing freeze-thaw seasons in northern high latitudes and associated influences on evapotranspiration. Hydrological Processes 25, 4142-4151, DOI:10.1002/hyp.8350.